RESEARCH ARTICLE

Physiological requirements for carbonate precipitation during biofilm development of *Bacillus subtilis etfA* mutant

Massimiliano Marvasi[1], Pieter T. Visscher[2], Brunella Perito[3], Giorgio Mastromei[3] & Lilliam Casillas-Martínez[1]

[1]Biology Department, University of Puerto Rico-Humacao, Humacao, PR, USA; [2]Department of Marine Sciences, Center for Integrative Geosciences, University of Connecticut, Groton, CT, USA; and [3]Dipartimento di Biologia Evoluzionistica, Università degli Studi di Firenze, Florence, Italy

Correspondence: Lilliam Casillas-Martínez, Biology Department, University of Puerto Rico-Humacao, Box CUH 100 Carr. 908, Humacao, PR 00791, USA. Tel.: +1 787 850 0000, ext. 9162; fax: +1 787 850 9439; e-mail: lilliam.casillas@upr.edu

Received 6 May 2009; revised 4 October 2009; accepted 20 October 2009.

DOI:10.1111/j.1574-6941.2009.00805.x

Editor: Julian Marchesi

Keywords
calcite precipitation; *etfA*; *Bacillus subtilis*; biofilm; B4 precipitation medium; EPS.

Abstract

Although the implications of calcium carbonate ($CaCO_3$) precipitation by microorganisms in natural environments are quite relevant, the physiology and genetics of this phenomenon are poorly understood. We have chosen *Bacillus subtilis* 168 as our model to study which physiological aspects are associated with $CaCO_3$ (calcite) formation during biofilm development when grown on precipitation medium. A *B. subtilis eftA* mutant named FBC5 impaired in calcite precipitation was used for comparative studies. Our results demonstrate that inactivation of *etfA* causes a decrease in the pH of the precipitation medium during biofilm development. Further analysis demonstrated that *eftA* extrudes an excess of 0.7 mol H^+ L^{-1} with respect to *B. subtilis* 168 strain. Using media buffered at different pH values, we were able to control calcite formation. Because *etfA* encodes the α-subunit of a putative flavoprotein involved in fatty acid metabolism, we compared the intracellular levels of NADH among strains. Our physiological assay showed that FBC5 accumulated up to 32 times more NADH than the wild-type strain. We propose that the accumulation of NADH causes a deregulation in the generation of the proton motive force ($\Delta\mu H^+$) in FBC5 producing the acidification.

Introduction

Mineralization, or mineral precipitation, is a widespread process among organisms. The mediation of mineralization by organisms is classified as either *controlled* or *induced* (Lowenstam & Weiner, 1989; Dupraz *et al.*, 2009a). In organisms such as multicellular eukaryotes, unicellular algae such as coccolithophores and diatoms and magnetotactic bacteria, the mineralization is defined as *controlled*; the mineralization process is controlled through intracellular organic matrices or vesicles and the process is thought to be under specific metabolic and genetic control (Lowenstam & Weiner, 1989; Bazylinski & Moskowitz, 1997; Bäuerlein, 2003, 2004). In contrast, *induced* mineralization is regulated by physiological activities and carried out in open environments (Lowenstam & Weiner, 1989; Ries *et al.*, 2008; Dupraz *et al.*, 2009b). This phenomenon is wide spread in the Bacterial Kingdom, and metabolic pathways such as photosynthesis, urea hydrolysis and sulfate reduction are all examples of *induced* mineralization (Chafetz & Buczynski, 1992; Hammes *et al.*, 2003; Dupraz & Visscher, 2005; Visscher & Stolz, 2005; Braissant *et al.*, 2007).

The ecological implications of bacterially *induced* biomineralization are various and several papers deal with biomineralization (Braissant *et al.*, 2004; Wright & Oren, 2005; Garvie, 2006; Dupraz *et al.*, 2009b). Moreover, the ecological relevance of *induced* mineralization such as microbial calcium carbonate ($CaCO_3$) precipitation has been exploited in biotechnology, with applications ranging from bioremediation to control leaching (Gollapudi *et al.*, 1995), plugging-cementation of rocks (Stocks-Fischer *et al.*, 1999), solid-phase capture of inorganic contaminants (Warren *et al.*, 2001) and the consolidation of carbonate materials of monuments (Barabesi *et al.*, 2003; Rodriguez-Navarro *et al.*, 2003). In all these applications, the genetics and physiology of the resident microorganisms are poorly understood. Here, we present a study of the physiology of $CaCO_3$ precipitation in a widely spread soil organism, *Bacillus subtilis*, which is an excellent candidate with a completely sequenced genome (Kunst *et al.*, 1997) and advanced characterization of its entire proteome (Wolff *et al.*, 2007).

Bacillus subtilis is able to produce calcite crystals in B4 precipitation medium (Boquet *et al.*, 1973). A gene cluster

FEMS MICROBIOLOGY ECOLOGY

involved in calcite precipitation was described in *B. subtilis* 168 strain (Barabesi *et al.*, 2007). The cluster contains five genes (*lcfA*, *ysiA*, *ysiB*, *etfB* and *etfA*), and five mutants carrying each of the five inactivated genes were constructed (FBC1–FBC5). All of these mutants, with the exception of FBC1 (mutated in *lcfA*), were unable to form calcite crystals on B4 solid precipitation medium. The *etfA* gene mutated in the strain named FBC5 was found to be essential for calcite precipitation (Barabesi *et al.*, 2007), and its product resembles an α-subunit of prokaryotic heterodimeric flavoproteins involved in electron transport during fatty acid metabolism. Even though it appears that the *etfA* gene is essential to form calcite crystals in *B. subtilis*, the physiology behind the impairment is unknown. In natural environments, several factors are linked to the absence of 'induced' crystal formation, for example pH variations, binding of calcium to extracellular polymeric substances (EPS) production of different quantities of EPS or production of EPS with different properties (Dupraz & Visscher, 2005; Wright & Oren, 2005; Wright & Wacey, 2005). The main goal of the current investigation was to understand the inability of *B. subtilis* FBC5 to produce crystals and the elucidation of the physiological pathways associated with the impairment.

Materials and methods

Bacterial strains and B4 precipitation medium

The strains used in this study were *B. subtilis* 168 (also called strain 168) (Anagnostopoulos & Spizizen, 1961) and *B. subtilis* 168 mutated in the *etfA* gene named strain FBC5 (Barabesi *et al.*, 2007). The cultures were routinely grown either on B4 solid or liquid precipitation medium (0.4% yeast extract, 0.5% dextrose, 0.25% calcium acetate and 1.4% agar in solid preparations) (Boquet *et al.*, 1973). FBC5 cultures were supplemented with 5 μg mL^{-1} chloramphenicol to maintain the selective pressure for maintaining the inserted plasmid. Unless otherwise specified, biofilms were grown on plates incubated at 37 °C inside a plastic bag to prevent dehydration.

Determination of growth kinetics, pH development and crystal formation in liquid cultures

Fifty milliliters B4 liquid medium was inoculated with 0.5 mL of strain 168 and FBC5 strains from overnight cultures and were placed in a 250-mL flask on a shaker incubator (120 r.p.m., 37 °C). Growth kinetics were reported by measuring the OD of the cultures until the stationary phase. To monitor crystal development, flasks containing cells at the beginning of the exponential phase ($OD_{600\,nm} = 0.3$) were incubated at 37 °C without shaking for up to a month. A control without cells was always incubated in parallel. The pH of the cultures was monitored using a pH meter (Hanna N2419). Hanna pH standard buffer solutions at pH 4.01 and 7.01 were used to calibrate the pH meter.

Crystal characterization and analyses

Crystal development in cultures was monitored using a dissecting microscope (Olympus SZX9), an optical microscope (Nikon Eclipse E400) and an environmental scanning electron microscope (ESEM) Quanta-200 FEI (with energy-dispersive spectroscopy). Crystals were collected and analyzed by X-ray diffractometry.

To verify the presence of a small carbonate precipitate (50–100 μm), a small sample of biofilm was treated with a drop of 1 N HCl on a glass slide. Gas production indicated the presence of crystals.

EPS extraction and Fourier transform infrared spectroscopy (FT-IR) analyses

EPS of strain 168 and FBC5 were recovered from their respective biofilms after 7 days of incubation on B4 medium according to Braissant *et al.* (2007). Biofilms were resuspended in sterile-distilled water and incubated in a shaker at 250 r.p.m. for 1 h at room temperature. Suspensions were centrifuged at 8000 ***g*** for 20 min at 4 °C. Supernatants were further filtered with a 0.45-μm nitrocellulose filter (Fisherbrand). The EPS in the filtrate was precipitated by adding cold ethanol (4 °C) in a 1 : 1 ratio, followed by an overnight precipitation at 4 °C. The EPS was recovered by centrifugation, placed in dialysis tubing (10 kDa) and dialyzed against deionized water. After dialysis, the EPS was stored at − 20 °C or freeze dried. FT-IR studies were carried out on freeze-dried samples using a Perkin-Elmer Spectrum 100 FT-IR spectrometer equipped with a single reflection Diamond/ZnSe Standard Universal ATR Accessory (Perkin-Elmer). Thirty-two scans were acquired for each sample. Experiments were conducted in duplicate.

pH changes during biofilm development

pH changes of *B. subtilis* grown on B4 plates were monitored using two pH indicators (Sigma Co.): bromothymol blue (BB), which transitions from yellow at pH 6.0 to blue at pH 7.6, and phenol red (PR), which exhibits a yellow color at pH 6.4 or below and a red color at pH 8.2 and above. BB and PR stock solutions (20 mg mL^{-1} in 0.1 N NaOH) were added to B4 medium before autoclaving at a final concentration of 0.0025% (v/v). Plates were inoculated by streaking a 4-cm line on the center of the plate and incubated at 37 °C for 1 week or until crystal formation. Experiments were replicated four times.

Test for $CaCO_3$ precipitation (*in vitro*)

To test the precipitation of $CaCO_3$ *in vitro*, we used two sets of plates with FBC5: one incubated for 24 h (no crystals) and the other incubated for 7 days. Both plates were placed inside a desiccator with 4 mL of ammonium hydroxide at room temperature for 24 h. As described above, crystal development was monitored using a dissecting microscope and a phase-contrast microscope (Nikon Eclipse E400). Experiments were replicated three times.

Precipitation test on modified B4 solid media at different pH

To test whether calcite formation was induced during biofilm development of strain 168 and FBC5 at different pH, the strains were grown on modified B4 plates prepared with final pH values ranging from pH 7.1 to pH 8.8. The pH of each plate was maintained by buffering the medium with Tris 1.2% (w/v) and 2 N HCl.

Urease activity test

Urease medium was prepared according to Washington (1981). Positive urease activity was indicated by an intense red color throughout the medium. *Escherichia coli* and *B. subtilis* 168 were used as negative and positive controls, respectively. Experiments were replicated three times.

Intracellular NADH assay

In order to test whether the mutation in *etfA* alters the total level of NADH, 50 mg of 168 and FBC5 biofilms were collected after 1, 2, 3 and 4 days of growth. The NADH content was assayed using the NAD^+/NADH quantification kit from BioVision Inc. Cells were washed with phosphate-buffered saline and disrupted by adding 0.2 g of glass beads and two cycles of 5 min in a Bead Beater (Fisher Co.) interrupted by 2-min intervals of cooling on ice. The disruption efficiency was monitored by protein quantification with Bradford Reagent (Sigma Co.). Cell extracts were filtered with a 10-kDa filter in order to remove any enzymes that might consume the released NADH. NADH concentration was expressed as ng NADH μg^{-1} proteins. The experiment was carried out with two replicas.

Results

Inactivation of the *eftA* gene does not affect calcite formation of *B. subtilis* in B4 liquid cultures

The growth kinetics, pH changes and crystal formation of strain 168 and FBC5 were compared on B4 liquid culture. No major differences were observed in the growth kinetics between 168 and FBC5 strains when grown in liquid medium (data not shown). Even though calcite formation in the FBC5 cultures was observed only after 1 month of incubations, crystals were formed by both strains once the pH of the culture exceeded 8.3 (Fig. 1a). X-ray diffraction analyses of crystals produced during growth in liquid media revealed calcite ($CaCO_3$) (Fig. 1b and c).

Crystals were observed by ESEM and compared with those formed during biofilm development (Fig. 2a). Interestingly, different morphologies were observed (Fig. 2b–e). Calcite crystals in Fig. 2b–d were organized around a central point to form spheroids. The flat circular shapes normally grow on the bottom of the flasks. Frequently, in the mutant aggregates of microspar-sized calcite crystals were present (Fig. 2e).

EPS secreted by *B. subtilis* strains during biofilm development share similar IR spectra

As calcite formation in *B. subtilis* was exclusive for strain 168 grown on solid medium, we decided to compare the EPS secreted by both biofilms grown on B4 solid medium. Although the peak distribution was similar to that previously reported for other *B. subtilis* strains (Omoike & Chorover, 2004), comparisons of the FT-IR spectra of the EPS from both strains tested in this study showed no major differences (Fig. 3).

The two FT-IR revealed an identical homology between the preparations and the presence of bands typical of proteins and carbohydrates. The broad band at 3282 could be assigned to OH stretching of alcohols. The presence of alcohols was confirmed in the band at 1045 (C-OH stretch) typically of cyclic alcohols and in the OH deformation band at 1376. The bands around 2924 were associated with C-H stretching of the sugar backbone, while the band at 1226 could be assigned to the stretching of the ether bonds C-O-C in the glycoside bond.

Two typical bands could be assigned to protein secondary structure: C = O of the amide I at 1637 and the amide II at 1547.

Decrease in pH during biofilm development of FBC5 is responsible for impairment in calcite formation

To investigate whether pH changes during biofilm development are associated with impairment of crystal formation in the *etfA* mutant (FBC5), both strains were grown on B4 solid medium supplemented with pH indicators. Interestingly, after 1 week of growth, strain FBC5 exhibited acidification in the medium (Fig. 4).

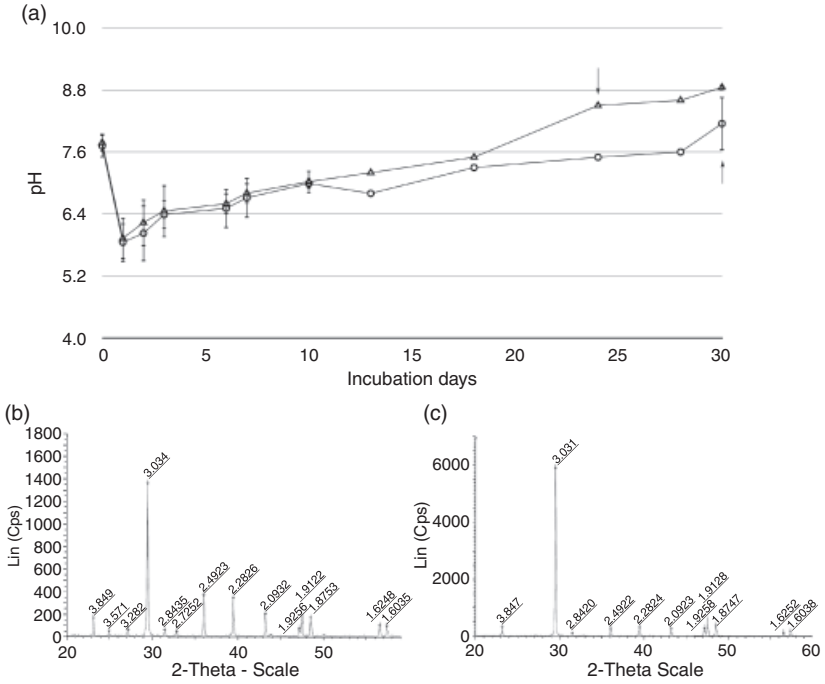

Fig. 1. The pH changes and calcite crystal formation in B4 liquid cultures of *Bacillus subtilis* 168 (△) and FBC5 strain (○). (a) Initial values indicate pH in starting cultures depicted by day 0. The bottles were further incubated without shaking for 1 month. pH values represent the mean of three experiments, with bars indicating SDs. Arrows indicate when calcite crystals were observed in each culture. (b, c) X-ray diffraction (XRD) diffractograms of crystals formed in B4 liquid cultures from *B. subtilis* 168 and FBC5, respectively. XRD analysis reveals calcite crystals for both the samples.

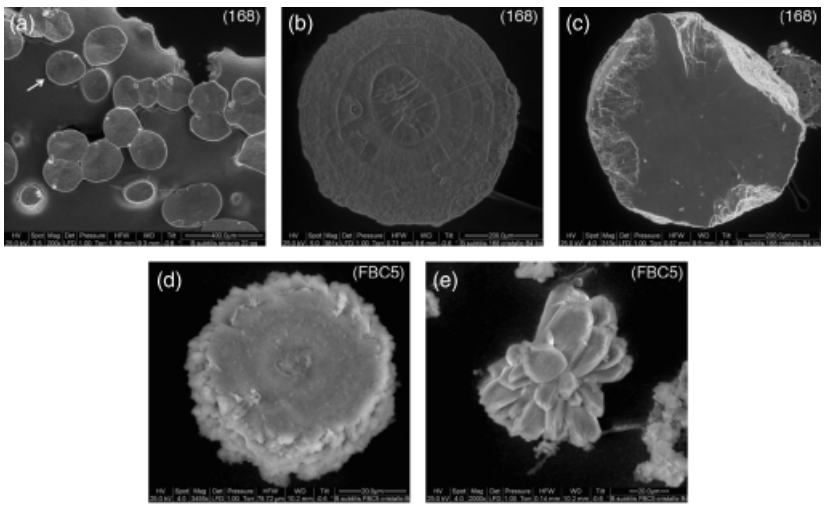

Fig. 2. ESEM micrographs revealing different morphologies of calcite crystals from *Bacillus subtilis* 168 and FBC5 cultures grown under different conditions. (a) Crystals present in biofilms from *B. subtilis* 168 after 1 week incubation. The white arrow indicates one of crystals in the biofilm. (b, c) Crystals formed in B4 liquid cultures from *B. subtilis* 168 after 1 month of incubation. (d, e) Crystals formed in B4 liquid cultures from strain FBC5 after 1 month of incubation.

Calcite crystal formation in *B. subtilis* biofilm is a reversible phenomenon

To test whether pH was indeed the main determinant in mineral precipitation, the pH of the medium was changed in order to investigate restoration of crystal formation. Two different experiments were conducted: in the first experiment, FBC5 biofilms were placed under an ammonium hydroxide-saturated headspace to determine whether a pH increase will initiate crystal formation (as a result of dissolution of ammonia into the plates). Crystal formation was restored within 24 h of incubation and coincided with a color transition in the BB plates to alkalinization. The resulting crystal morphology was different compared with *B. subtilis* 168 grown on standard B4 plates (Fig. 5a and b) as observed in liquid cultures (Fig. 2).

In the second experiment, strain FBC5 was streaked on modified B4 medium containing BB and buffered using either 0.6% or 1.2% w/v of Tris, pH = 8.3. Crystal formation on FBC5 was re-established after 1 week of incubation of the

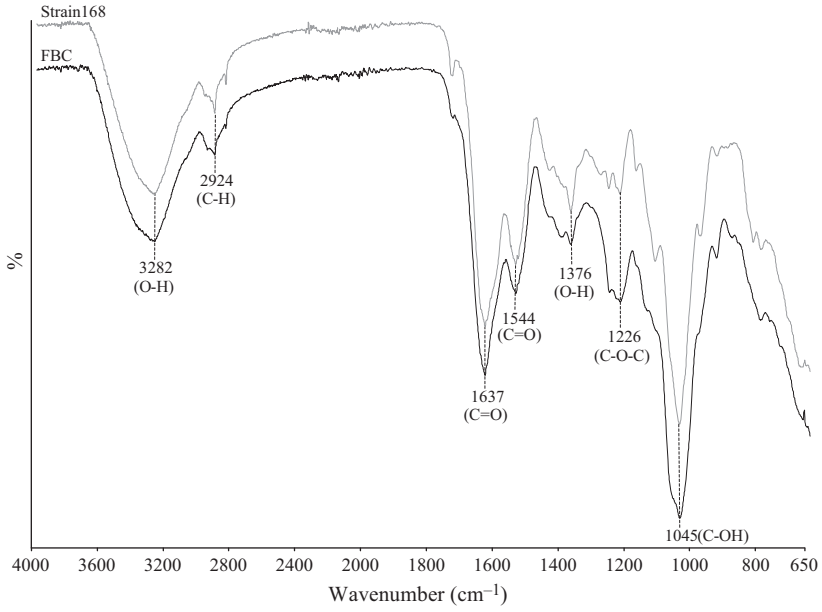

Fig. 3. FT-IR spectra of EPS from *Bacillus subtilis* 168 and FBC5 biofilms after 1 week of incubation at 37 °C. Upper spectrum, *B. subtilis* 168; lower spectrum, strain FBC5. FT-IR were conducted in replicas for each strain revealing identical peak patterns among preparations.

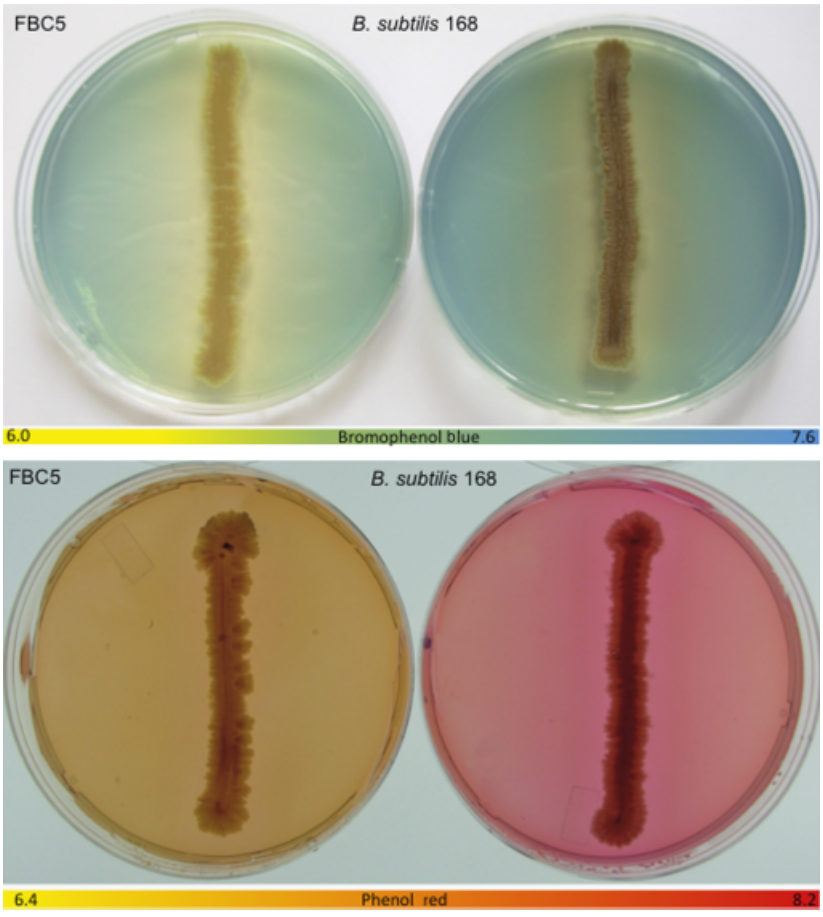

Fig. 4. Changes in pH of *Bacillus subtilis* 168 and strains FBC5 grown on B4 solid medium supplemented with BB and PR after 1 week of incubation at 37 °C. Bottom colored bars represent the gradient of color change associated with pH values for the indicators BB and PR (colors in the bars are only indicative). Replicas for each strain were always identical.

plates containing 1.2% Tris (Fig. 5c and d) and no crystals were formed on the plates with 0.6% Tris. Similarly, changes in BB indicator plates were only evident in the 0.6% plates, but not those supplemented with 1.2% of Tris (data not shown), indicating that in the presence of 1.2% of Tris, FBC5 was unable to acidify the microenvironment of the

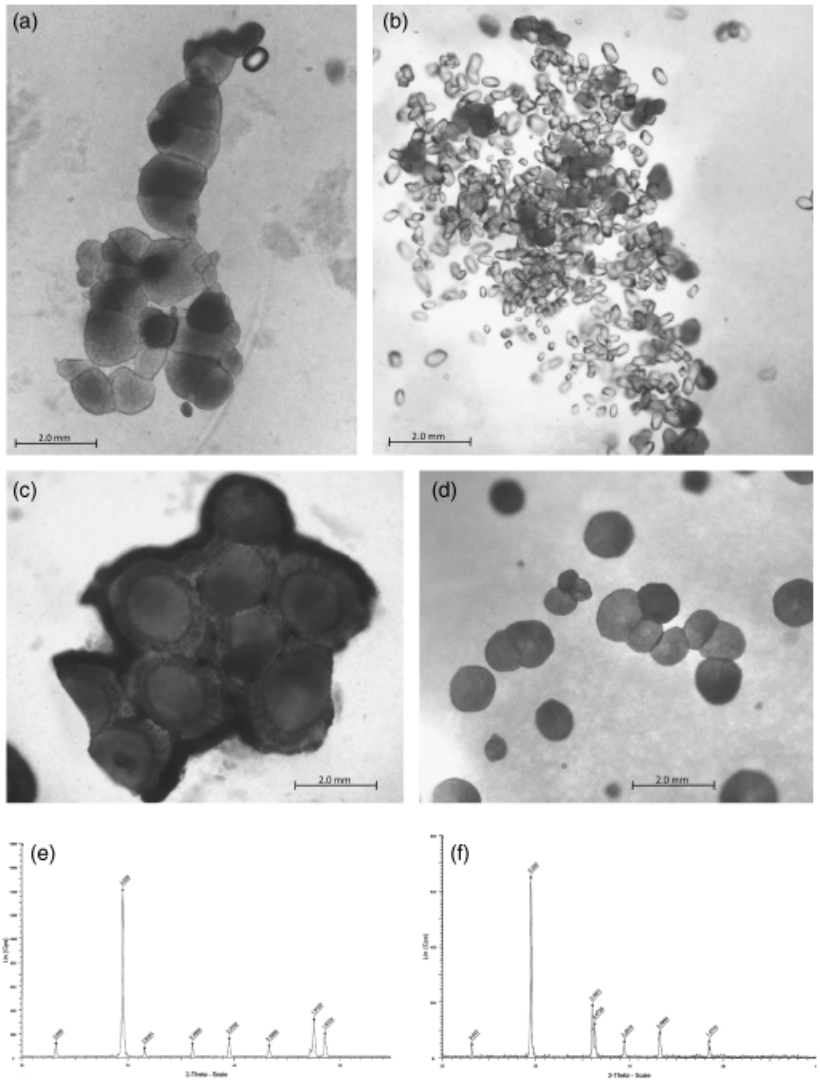

Fig. 5. Calcite formation in *Bacillus subtilis* strains 168 and FCB5 grown under different conditions. (a) Optical microscopic image of crystals from *B. subtilis* 168 after 1 week of incubation at 37 °C in B4 plates (no crystals were formed from plates inoculated with FBC5 under similar conditions). (b) Optical microscopic image of calcite crystals from FBC5 biofilm incubated in ammonium hydroxide-saturated headspace; crystals were formed within 24 h. Optical microscopic images of calcite crystals were also obtained from *B. subtilis* 168 (c) and FBC5 (d) on B4 plates supplemented with Tris 1.2%, pH 8.3. (e, f) X-ray diffraction (XRD) diffractograms of crystals formed on B4 plates supplemented with Tris 1.2%, pH 8.3, from *B. subtilis* 168 and FBC5, respectively. The XRD analysis reveals that calcite is present in both the samples. Diffractogram from sample (f) shows additional peaks at 36.3°.

biofilm. X-ray diffraction analyses of crystals produced during growth on solid B4 1.2% Tris, pH 8.3, revealed calcite (Fig. 5e and f).

FBC5 mutant extrudes 0.7 mol H^+ L^{-1} more than strain 168 on precipitating media

To estimate the differences in proton extrusion among *B. subtilis* strains, we compared their capacity to produce carbonate crystals on well-buffered B4 medium plates (supplemented with 1.2% Tris). The pH of the plates used ranged from 7.1 to 8.8. As depicted in Fig. 6, calcite formation by *B. subtilis* strain 168 started at pH 7.5, while its FBC5 mutant was only able to form crystals when the pH was at 8.2. Consequently, the proton extrusion by strain FBC5, indicated by the double arrow, was responsible for the difference in the pH values required for crystal formation on plates inoculated with strain 168 and FBC5. Using the pH value of 8.2 for FBC5 and pH 7.5 for strain 168 at which precipitation commenced, we determined that $10^{-7.5} - 10^{-8.2} = 2.5 - 1.8\ \text{mol}\ L^{-1} = 0.7\ \text{mol}\ H^+\ L^{-1}$ more were extruded by strain FBC5 when compared with strain 168. However, this estimation could not take into account all the various components of the B4 medium. Therefore, it is likely that the FBC5 strain extrudes even more protons than calculated.

Sources for the excess of proton extrusion in FBC5

The excess of proton extrusion observed for strain FBC5 can be due to lack of OH^- production or, alternatively, excess of H^+ production. We tested both possibilities. For the scenario in which OH^- is removed, we tested the urease presence of

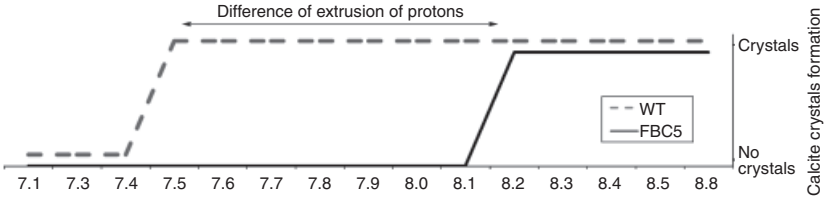

Fig. 6. Estimated differences in proton extraction by each strain based on the capacity of crystal formation during growth on modified B4 (pH 7.1–8.8) of *Bacillus subtilis* 168 strain and FBC5. The double-arrow represents the difference in proton extrusion by FBC5 due to the mutation in *etfA*. Results from triplicate samples analyzed for each strain were always identical.

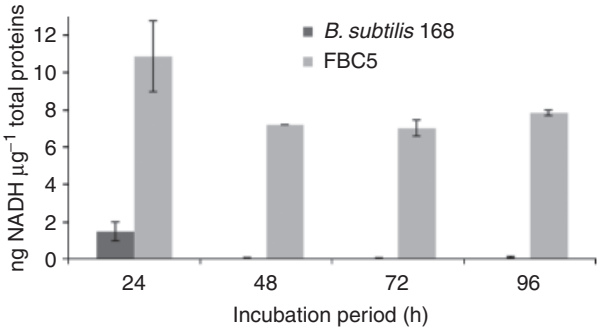

Fig. 7. Comparison of intracellular levels of NADH in *Bacillus subtilis* strain 168 and *etfA* mutant grown on B4 plates incubated at 37 °C. Bars represent the SD.

both strains to check whether a difference in ammonia production in the mutant caused the lower pH as shown in the following equations (Hammes *et al.*, 2003):

$$CO(NH_2)_2 + H_2O \rightarrow NH_2COOH + NH_3 \quad (1)$$

$$NH_3 + H_2O \rightarrow NH_4^+ + OH^- \quad (2)$$

Both strains were positive to the urease test. However, a different result was reported when the production of H^+ was studied.

Increase in the intracellular levels of NADH in the *B. subtilis* FBC5 mutant during calcite formation

In *B. subtilis*, *eftA* encodes a putative α-subunit of a flavoprotein involved in fatty acid metabolism. The function of EftA protein seems to be related to the oxidation–reduction reactions of NAD^+/NADH (De Mendoza *et al.*, 2002; Fujita *et al.*, 2007; Inui *et al.*, 2008), and by extension, may influence the accumulation of H^+. Determination of intracellular levels of NADH during biofilm development showed that cells with the *eftA* mutation accumulated more NADH than the strain 168 (Fig. 7). Between the second and the fourth days, the intracellular levels of NADH were about 32 times higher in FBC5 than the strain 168.

Discussion

Previously, Barabesi *et al.* (2007) identified an operon involved in calcite precipitation. They reported that the last gene of the operon, *etfA*, which encodes a putative flavoprotein, was found to be essential for the precipitation process on solid medium. In the current study, we have focused on the physiology of the *eftA* mutant in order to understand the lack of calcite crystal formation. In a natural environment, calcium-binding sites (i.e. EPS), pH, $[Ca^{2+}]$, $[CO_3^{2-}]$ as well as the spatial distribution of these ions/molecules are key players in calcite precipitation (Dupraz & Visscher, 2005; Dupraz *et al.*, 2009a). Consequently, we studied whether calcite formation phenomenon was exclusive of solid cultures. Growth comparison between 168 and FBC5 strains in liquid cultures revealed no major differences in the growth kinetics, change in pH and calcite formation (Fig. 1). X-ray diffraction analyses of crystals produced during growth in liquid media revealed calcite composition (Fig. 1b and c). Barabesi *et al.* (2007) monitored the pH of cultures of strains 168 and FBC5 for 10 days in B4 liquid medium with calcium acetate replaced by sodium acetate without detecting significant differences among strains. We concluded that the impairment in calcite precipitation was only related to solid medium probably due to the particular spatial microenvironmental conditions in the biofilm. Preliminary analysis of EPS extracted from both biofilms revealed similar FT-IR patterns in strains 168 and FBC5 (Fig. 3). However, major differences were observed in pH variations; acidification of plates coincided only during biofilm development by strain FBC5 (Fig. 4). The decrease in the pH of FBC5 biofilms was the main process responsible for the lack of calcite crystal formation. The phenomenon was reversible and calcite crystal formation was restored when the biofilm was incubated under alkaline conditions, either under an ammonium hydroxide headspace or on plates buffered with 1.2% Tris ($pH \geq 8.2$) (Fig. 5a–d). However, these data suggest that no specific inhibitors of precipitation are produced. Regulation of precipitation by the local pH was further confirmed using media buffered at different pH values, through which we were able to control the calcite crystal formation in biofilms (Fig. 6). The current findings are similar to those

reported for $CaCO_3$ precipitation by heterotrophic bacteria (Chafetz & Buczynski, 1992; Rivadeneyra *et al.*, 1999). When provided with sufficiently high $[Ca^{2+}]$, heterotrophic bacteria can precipitate $CaCO_3$ if the system is very well buffered, and so without a change in pH, an increase in CO_2/HCO_3^- causes an increase in $[CO_3^{2-}]$ (Visscher & Stolz, 2005).

When considering organic carbon metabolism only, bacteria capable of aerobic-heterotrophic respiration and fermentation dissolve, rather than precipitate $CaCO_3$ (Visscher & Stolz, 2005). *Bacillus subtilis* metabolism can be described by either of these two metabolic types. However, microorganisms that display ureolytic activity, as well as *B. subtilis*, are capable of precipitating calcite crystals (Hammes *et al.*, 2003). Urea hydrolysis is one of the metabolic processes that enhances microbial carbonate precipitation in natural environments such as soil (Hammes *et al.*, 2003), principally through OH^- production [see Eqn. (1) and (2)]. If the FBC5 mutant lacked the capacity to hydrolyze urea, this could account for the lack of $CaCO_3$ precipitation. Curiously, no differences (in terms of color variation of the medium) in urease activity were found between *B. subtilis* strain 168 and strain FBC5. We propose that the actual mechanism decreasing the pH during FBC5 biofilm development resulted from H^+ production exceeding that of OH^-. Specifically, the H^+ extruded by the mutant was estimated to be $0.7\ H^+\ mol\ L^{-1}$ more compared with strain 168 (Fig. 6), and the excess of protons could result from a misregulation in some part of the EtfA pathway. Even though the function of the two EtfA–B proteins in *B. subtilis* is only putative, in *Clostridium acetobutylicum*, *etfA* and *etfB* coexpression is essential for the butyryl-CoA dehydrogenase activity, and *etfA–B* genes are involved in the oxidation of NADH in the butyryl-CoA synthesis pathway (Inui *et al.*, 2008). Sequence similarity analysis of EtfA–B proteins of *C. acetobutylicum* showed 64% and 57% similarity to EtfA–B proteins in *B. subtilis*, respectively.

If the reduction of β -hydroxybutyryl-CoA takes place in *B. subtilis* in a similar manner as in *C. acetobutylicum*, we expected to see an increase in NADH accumulation. Cytoplasmic levels of NADH increased up to 37 times in the strain FBC5 compared with the strain 168 (Fig. 7). We hypothesize that a possible link exists between proton extrusion and the cytosolic accumulation of NADH in *B. subtilis*. NADH dehydrogenase of *B. subtilis*, even though its function in transmembrane proton pumping is unknown, plays an important role in catalyzing the translocation of electrons from NADH to menaquinone, thereby generating a proton-motive force, which can be utilized to produce ATP for cellular metabolism (Mitchell, 1961; Sone *et al.*, 2004; Gyan *et al.*, 2006). NADH (and NADPH) oxidation results in the generation of a proton-motive force across the vesicle membrane, which drives the uptake of solutes such as dicarboxylic acids (Bisschop *et al.*, 1975; Bergsma *et al.*, 1981). We propose that the accumulation of NADH in FBC5 could be involved in the generation of a proton gradient through the respiratory electron transport.

Differences in calcite crystal morphologies between 168 and FBC5 strains

As reported previously, crystal morphology depends on the growth conditions and the *B. subtilis* strain used. Different morphologies were reported by 168 and FBC5 strains grown in liquid culture (Fig. 2b–e), under ammonium headspace on plates (Fig. 5a and b) as well as on the plates buffered at pH 8.3 (Fig. 5c and d). Crystal morphology resulting from microbial precipitation may be affected by differences in EPS properties such as concentration, acidity, functional group composition and pH (Braissant *et al.*, 2003). Even though the FT-IR peak distribution was similar for EPS isolated from strains 168 and FBC5, further quantitative experimentations are required to determine whether differences in protein composition and abundance, acidic groups and sugar composition could influence calcite crystal morphology.

Advantages of an *in vitro* system

Microorganisms grown in the laboratory under controlled conditions can delineate their ability to alter the geochemistry of the microenvironment (Baskar *et al.*, 2006). However, it is important to evaluate the relevance of mineral precipitation experiments on plates, whose utility until now may have been underestimated. The current study demonstrates that (1) the generation of mutant strains enables a study of the genes and metabolic reactions involved in the precipitation of calcite crystals; (2) it is possible to compare the difference in proton production between two or more carbonate-precipitating strains and assess their effect on calcite mineral precipitation; (3) an appropriate experimental design allows the control of the geochemical fluctuation (i.e. of Ca^{2+}, pH, etc.) within the system; and (4) *in vitro* experiments facilitate study of the mineralogy and morphology of mineral precipitates (Lian *et al.*, 2006; Braissant *et al.*, 2007; Ercole *et al.*, 2007).

Acknowledgements

We acknowledge Dr Ezio Fasoli from the Chemistry Department at the University of Puerto Rico-Humacao for help with the FT-IR. We also thank Dr Cristiana Giordano from CEME Centro di Microscopie Elettroniche, Florence, Italy, for the ESEM micrographs. This work was supported by the following grants: NSF MCB 0137336 to P.T.V. and L.C.-M., USDA CREEST 2007 to L.C.-M., NSF EAR 0221796 and 0331929 to P.T.V. Partial support for undergraduate students helping in the project was provided by the MARC

program. This is UConn's Center for Integrative Geosciences contribution number 16.

References

Anagnostopoulos C & Spizizen J (1961) Requirements for transformation in *Bacillus subtilis*. *J Bacteriol* **81**: 741–746.

Barabesi C, Tamburini E, Mastromei G & Perito B (2003) Mechanisms of microbial calcium carbonate precipitation. *Art, Biology, and Conservation: Biodeterioration of Works of Art* (Koestler RJ, Koestler VH, Charola AE & Nieto-Fernandez FE, eds), pp. 472–485. Metropolitan Museum of Art, New York.

Barabesi C, Galizzi A, Mastromei G, Rossi M, Tamburini E & Perito B (2007) *Bacillus subtilis* gene cluster involved in calcium carbonate biomineralization. *J Bacteriol* **189**: 228–235.

Baskar S, Baskar R, Mauclaire L & McKenzie JA (2006) Microbially induced calcite precipitation in culture experiments: possible origin for stalactites in Sahastradhara caves, Dehradun, India. *Curr Sci India* **90**: 58–64.

Bäuerlein E (2003) Biomineralization of unicellular organisms: an unusual membrane biochemistry for the production of inorganic nano- and microstructures. *Angew Chem Int Edit* **42**: 614–641.

Bäuerlein E (2004) *Biomineralization. Progress in Biology, Molecular Biology and Application*. Wiley-VHC Verlag GmbH & Co., Weinheim, Germany.

Bazylinski DA & Moskowitz BM (1997) Microbial biomineralization of magnetic iron minerals; microbiology, magnetism and environmental significance. *Rev Mineral Geochem* **35**: 181–223.

Bergsma J, Strijker R, Alkema JYE, Seijen HG & Konings WN (1981) NADH dehydrogenase and NADH oxidation in membrane vesicles from *Bacillus subtilis*. *Eur J Biochem* **120**: 599–606.

Bisschop A, Doddema H & Konings WN (1975) Dicarboxylic acid transport in membrane vesicles from *Bacillus subtilis*. *J Bacteriol* **124**: 613–622.

Boquet E, Boronat A & Ramos-Cormenzana A (1973) Production of calcite (calcium carbonate) crystals by soil bacteria is a general phenomenon. *Nature* **246**: 527–529.

Braissant O, Cailleau G, Dupraz C & Verrecchia EP (2003) Bacterially induced mineralization of calcium carbonate in terrestrial environments: the role of exopolysaccharides and amino acids. *J Sediment Res* **73**: 485–490.

Braissant O, Cailleau G, Aragno M & Verrecchia EP (2004) Biologically induced mineralization in the tree *Milicia excelsa* (Moraceae): its causes and consequences to the environment. *Geobiology* **2**: 59–66.

Braissant O, Decho AW, Dupraz C, Glunk C, Przekop KM & Visscher PT (2007) Exopolymeric substances of sulfate-reducing bacteria: interactions with calcium at alkaline pH and implication for formation of carbonate minerals. *Geobiology* **5**: 401–411.

Chafetz HS & Buczynski C (1992) Bacterially induced lithification of microbial mats. *Palaios* **7**: 277–293.

De Mendoza D, Schujman GE & Aguilar PS (2002) Biosynthesis and function of membrane lipids. *Bacillus subtilis and Closest Relatives* (Soneshein AL, ed), pp. 43–56. ASM Press, Washington, DC.

Dupraz C & Visscher PT (2005) Microbial lithification in marine stromatolites and hypersaline mats. *Trends Microbiol* **13**: 429–438.

Dupraz C, Reid RP, Braissant O, Decho AW, Norman RS & Visscher PT (2009a) Processes of carbonate precipitation in modern microbial mats. *Earth-Sci Rev* **96**: 141–162.

Dupraz S, Parmentiera M, Méneza B & Guyota F (2009b) Experimental and numerical modeling of bacterially induced pH increase and calcite precipitation in saline aquifers. *Chem Geol* **265**: 44–53.

Ercole C, Cacchio P, Botta AL, Centi V & Lepidi A (2007) Bacterially induced mineralization of calcium carbonate: the role of exopolysaccharides and capsular polysaccharides. *Microsc Microanal* **13**: 42–50.

Fujita Y, Matsuoka H & Hirooka K (2007) Regulation of fatty acid metabolism in bacteria. *Mol Microbiol* **66**: 829–839.

Garvie L (2006) Decay of cacti and carbon cycling. *Naturwissenschaften* **93**: 114–118.

Gollapudi UK, Knutson CL, Bang SS & Islam MR (1995) A new method for controlling leaching through permeable channels. *Chemosphere* **30**: 695–705.

Gyan S, Shiohira Y, Sato I, Takeuchi M & Sato T (2006) Regulatory loop between redox sensing of the NADH/NAD^+ ratio by Rex (YdiH) and oxidation of NADH by NADH dehydrogenase Ndh in *Bacillus subtilis*. *J Bacteriol* **188**: 7062–7071.

Hammes F, Boon N, de Villiers J, Verstraete W & Siciliano SD (2003) Strain-specific ureolytic microbial calcium carbonate precipitation. *Appl Environ Microb* **69**: 4901–4909.

Inui M, Suda M, Kimura S *et al.* (2008) Expression of *Clostridium acetobutylicum* butanol synthetic genes in *Escherichia coli*. *Appl Microbiol Biot* **77**: 1305–1316.

Kunst F, Ogasawara N, Moszer I *et al.* (1997) The complete genome sequence of the gram-positive bacterium *Bacillus subtilis*. *Nature* **390**: 249–256.

Lian B, Hua Q, Chena J, Jia J & Teng HH (2006) Carbonate biomineralization induced by soil bacterium *Bacillus megaterium*. *Geochim Cosmochim Ac* **22**: 5522–5535.

Lowenstam HA & Weiner S (1989) *On Biomineralization*. Oxford University Press, New York.

Mitchell P (1961) Coupling of phosphorylation to electron and hydrogen transfer by a chemi-osmotic type of mechanism. *Nature* **191**: 144–148.

Omoike A & Chorover J (2004) Spectroscopic study of extracellular polymeric substances from *Bacillus subtilis*: aqueous chemistry and adsorption effects. *Biomacromolecules* **5**: 1219–1230.

Ries JB, Anderson MA & Hill RT (2008) Seawater Mg/Ca controls polymorph mineralogy of microbial $CaCO_3$: a potential proxy for calcite–aragonite seas in Precambrian time. *Geobiology* **6**: 106–119.

Rivadeneyra MA, Delgado G, Soriano M, Ramos-Cormenzana A & Delgado R (1999) Biomineralization of carbonates by *Marinococcus albus* and *Marinococcus halophilus* isolated from the Salar de Atacama (Chile). *Curr Microbiol* **39**: 53–57.

Rodriguez-Navarro C, Rodriguez-Gallego M, Ben Chekroun K & Gonzalez-Munoz MT (2003) Conservation of ornamental stone by *Myxococcus xanthus*-induced carbonate biomineralization. *Appl Environ Microb* **69**: 2182–2193.

Sone N, Hägerhäll C & Sakamoto J (2004) Respiration in archaea and bacteria: diversity of prokaryotic respiratory systems. *Respiration in Archaea and Bacteria*, *Vol. 16* (Zannoni D, ed), pp. 36–57. Springer, Berlin.

Stocks-Fischer S, Galinat JK & Bang SS (1999) Microbiological precipitation of $CaCO_3$. *Soil Biol Biochem* **31**: 1563–1571.

Visscher PT & Stolz JF (2005) Microbial mats as bioreactors: populations, processes, and products. *Palaeogeogr Palaeocl* **219**: 87–100.

Warren LA, Maurice PA, Parmar N & Ferris FG (2001) Microbially mediated calcium carbonate precipitation: implications for interpreting calcite precipitation and for solid-phase capture of inorganic contaminants. *Geomicrobiol J* **18**: 93–115.

Washington JA (1981) *Laboratory Procedures in Clinical Microbiology*. Springer-Verlag, New York, NY.

Wolff S, Antelmann H, Albrecht D *et al.* (2007) Towards the entire proteome of the model bacterium *Bacillus subtilis* by gel-based and gel-free approaches. *J Chromatogr B* **849**: 129–140.

Wright DT & Oren A (2005) Nonphotosynthetic bacteria and the formation of carbonates and evaporites through time. *Geomicrobiol J* **22**: 27–53.

Wright DT & Wacey D (2005) Precipitation of dolomite using sulphate-reducing bacteria from the Coorong Region, South Australia: significance and implications. *Sedimentology* **52**: 987–1008.